

THE LOCATION OF THE SUBSOLAR BOW SHOCK OF VENUS: IMPLICATIONS FOR THE OBSTACLE SHAPE

C. T. Russell, J. G. Luhmann and J. L. Phillips

Institute of Geophysics and Planetary Physics, University of California,
Los Angeles, California 90024

Abstract. The rise in periapsis altitude with time has allowed the Pioneer Venus spacecraft to begin probing the subsolar Venus bow shock. This has allowed the altitude of the subsolar bow shock to be determined by in situ observations for the first time. The observed altitude of 2280 km at the nose together with the previously determined terminator altitude can be used to infer the shape of the obstacle using the gas dynamic model of the solar wind interaction with Venus. When this shape is compared to the measured locations of the Venus ionopause (defined as the point where the magnetosheath magnetic field pressure and ionospheric thermal pressures are equal), it is found that the observed ionopause position is too low to qualify as the obstacle. We infer that a layer of the mass loaded plasma in the magnetosheath forms the magnetic barrier.

Introduction

The precise location of the subsolar Venus bow shock has been difficult to determine because few in situ observations of the bow shock are available at low solar zenith angles. This lack of observations is due to the geometry of the orbits of the Venera 9, 10 and Pioneer Venus spacecraft. However, recently the gradual evolution of the Pioneer Venus orbit has permitted a detailed examination of this region. The latitude of periapsis has decreased to lower latitudes and the altitude of periapsis has risen so that now it is often in the solar wind as it passes the subsolar point and not in the planetary magnetosheath.

A determination of the precise location of the subsolar bow shock is of some interest because initial studies of the bow shock appeared to indicate that the nose of the shock might be closer to the planet than expected and that this closeness might indicate some absorption of the solar wind by the planet (Russell, 1977). This early study used the flyby data from Mariner 5 and 10 and Venera 4 and 6. One measurement from Venera 9 was also used. Later analyses of a much larger data set from Venera 9 and 10 appeared to confirm the closeness of the subsolar bow shock (Smirnov et al., 1980). The former study found an extrapolated range of subsolar bow shock altitudes of 540-1940 km while the latter found a range of 1290-1790 km.

Most of the data used in these studies were obtained at large solar zenith angles near the terminator and beyond. The location and shape of the shock was determined accurately in the

near terminator region and then extrapolated to the subsolar point. This technique is sensitive to the distribution of data chosen and the fitting procedure unless there is a significant amount of data actually in the subsolar region. Slavin et al. (1979) took some care in this regard and obtained an altitude of 2100 km. In a later study they obtained a value of 2300 to 2600, with the lower number preferred (Slavin et al., 1980). Since there is some discrepancy in these extrapolated values, since the data to resolve this controversy are now available and since resolving this question has implications for the nature of the solar wind interaction with Venus, we examine below the observed and expected location of the Venus bow shock.

Observations

In the subsolar region, the trajectory of Pioneer Venus is nearly parallel to the shock surface in the subsolar region. When the orbit is close to the expected position of the bow shock as it is at present, the variable size of the bow shock causes the subsolar trajectory to either lie entirely inside the magnetosheath, lie entirely out in the solar wind or to be replete with multiple shock crossings. In the latter case the observed crossings lie along the trajectory and not necessarily at the average location of the bow shock. In order to determine an average shock position a different approach is necessary than the traditional one of using observed crossing locations. Instead we characterized each minute of near subsolar data as to whether the spacecraft was in the magnetosheath or solar wind. The last three subsolar passes were used: orbits 1739-1800, 1941-2002 and 2181-2229. The trajectory was rotated into aberrated solar wind coordinates and the percent of time spent in the magnetosheath was calculated as a function of altitude and solar zenith angle. The data were first binned in boxes of dimension 200 km in altitude by 3° in solar zenith angle and smoothed twice with a two-dimensional Gaussian filter. Next the altitude of the median and upper and lower quartiles of magnetosheath residence were calculated and are plotted in Figure 1 as a function of solar zenith angle. We estimate this procedure is accurate to ± 50 km.

As Figure 1 shows, the subsolar shock is usually at an altitude of 2280 km but 25% of the time can be lower than 2080. We cannot determine the upper quartile at the subsolar point but estimate from observations away from the subsolar point that the upper quartile is symmetric with the lower quartile. Thus we expect that 25% of the time the bow shock is above 2480 km at the subsolar point. This result agrees fairly closely with the 2300 km distance previously inferred by Slavin et al. (1980).

Copyright 1985 by the American Geophysical Union.

Paper number 5L6655.

0094-8276/85/005L-6655\$03.00

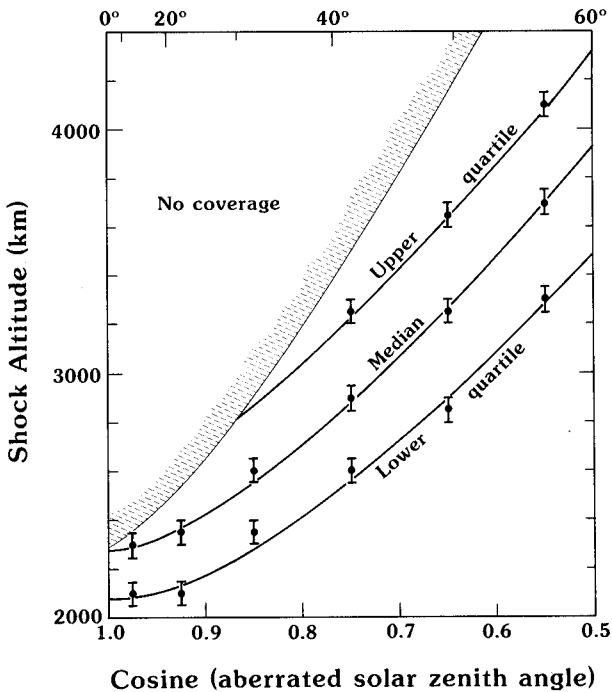


Fig. 1. The altitude of the Venus bow shock as a function of solar zenith angle. Upper and lower quartiles are also given where available. No data have yet been obtained in the upper left-hand corner of the diagram.

Inferred Obstacle Shape

The shock standoff distance is sensitive to both the Mach number of the free stream solar wind and the obstacle size and shape. For a Mach number of 4.5, which is most appropriate for Venus (Tatrallyay et al., 1984) and a ratio of specific heats of 5/3, the gas dynamic code of

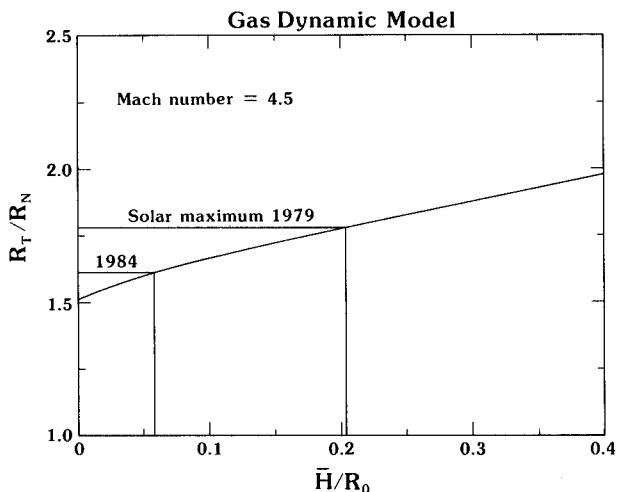


Fig. 2. The ratio of the shock radius at the terminator to the shock radius at the nose as a function of the gravitationally adjusted scale height of the ionosphere measured in terms of planetary radii using the gas dynamic model of Spreiter and Stahara (1980). A Mach number of 4.5 and a ratio of specific heats of 5/3 has been used.

Spreiter and Stahara (1980) can be used to calculate shock shapes for different obstacle shapes. We use a ratio of specific heats of 5/3 because this value gives the best standoff distance for the terrestrial shock when the correct shape of the magnetopause is used (Fairfield, 1971). Furthermore, we find that this value gives the best agreement between observations and predictions from the Rankine-Hugoniot equations for both interplanetary shocks (Russell et al., 1983) and bow shocks (Winterhalter et al., 1985). The obstacle shapes are characterized by the ratio of the ionospheric scale height to the planetary radius \bar{H}/R_0 where \bar{H} takes the variation of gravitational potential with altitude into account. If the ratio of the terminator radius of the shock R_T to the nose radius R_N is used as a measure of shape, the gas dynamic code gives the result shown in Figure 2. Alexander and Russell (1985) have previously found the average terminator distance to the shock at this epoch to be approximately 2.22 R_V . With a nose distance of 1.38, this gives an observed R_T/R_N of 1.61 which is indicated in Figure 2. It is seen that an obstacle with an $\bar{H}/R_0 = .06$ will produce the observed shock shape. On the other hand, if we assume that the subsolar shock location is constant over the solar cycle, then the terminator crossing distance of 2.45 R_V seen at solar maximum (Alexander and Russell, 1985) implies that at that time the value of \bar{H}/R_0 was 0.2. As will be shown below, this represents a significant change in shape of the obstacle.

While we do not have measurements of the location of the subsolar bow shock in 1979, our best extrapolation from the near terminator data give a subsolar shock location of 2300 km (Slavin et al., 1980) which is insignificantly different than our value of 2280 km obtained in 1984.

Figure 3 shows the distance from the nose of the shock to the obstacle for varying \bar{H}/R_0 . For our inferred solar maximum shape corresponding to \bar{H}/R_0 of 0.2, the standoff distance D is 0.32 obstacle radii, R_{Obs} . For an \bar{H}/R_0 of 0.06 the standoff distance is 0.26 R_{Obs} . These correspond

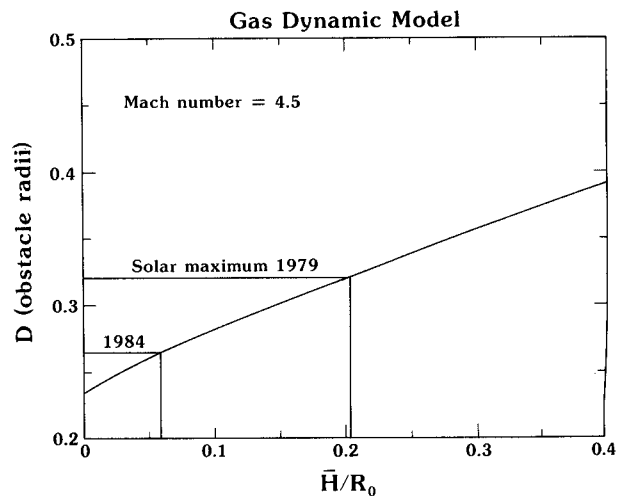


Fig. 3. The distance from the obstacle to the bow shock at the subsolar point as a function of the gravitationally adjusted scale height of the ionosphere using the gas dynamic model of Spreiter and Stahara.

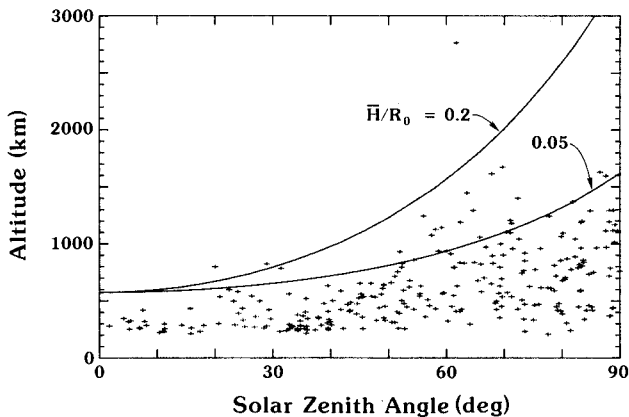


Fig. 4. The shape of the effective obstacle at solar maximum and near solar minimum plotted versus solar zenith angle. Also shown are the locations of the pressure balance ionopause (Phillips et al., 1984).

to effective obstacle altitudes of 275 km at solar maximum and 576 km near solar minimum. Since the effective altitude of the obstacle to the solar wind flow can be larger than the altitude of the ionopause because of the effects of mass loading, we consider the 576 km obstacle altitude as entirely plausible. On the other hand, the smaller altitude at solar maximum seems counter-intuitive. We would expect the obstacle to be larger at solar maximum if only because of greater solar heating of the atmosphere and ion production in the ionosphere. If we adopt instead an assumption of constant obstacle radius at the subsolar point, we can use Figures 2 and 3 to deduce that the shape parameter should be about 0.17 and the subsolar shock distance about 2600 km at solar maximum.

Figure 4 shows the shape of the effective obstacle for $\bar{H}/R_0 = 0.05$ and 0.2 starting at a constant subsolar obstacle altitude. This illustrates the very large change in shape that occurs over the solar cycle. The points drawn are those of the pressure balance ionopause, obtained at solar maximum. The pressure balance ionopause, the point where the magnetic and plasma pressures are equal, is almost always below the altitude of the effective obstacle corresponding to solar maximum. If we assume that the difference between the ionopause and the obstacle altitude is due to a mass loading effect, so that there a magnetic barrier is formed, then the barrier thickness ranges from about 250 km at the subsolar point to about 800 km at solar minimum at the terminator and 2500 km at solar maximum.

Discussion

We have used the gas dynamic model assuming that for the average Mach number of the solar wind at Venus of 4.5, the gas dynamic model provides an accurate representation of shock location. While this may not be precisely true we do expect that we can trust the qualitative inferences from the data. Using the model to infer changes in the shape of the effective planetary obstacle, we find that the shape changes drastically during the solar cycle. The shape is very magnetosphere-like at solar maximum

and very ionospheric in shape near solar minimum. We attribute this difference to the varying effects of mass loading.

The inferred obstacle size is significantly larger than the observed ionopause, either that defined by Brace et al. (1980) or by Phillips et al. (1984). We do not have a measure of the size of the ionopause in 1984 near solar minimum but we expect it to be similar to that observed at solar maximum.

We note that since the obstacle size is larger than the size of the ionopause, we do not need to invoke absorption to explain our results as was done previously (Russell, 1977; Slavin et al., 1983). The difference between this study and that of Russell (1977) is that better measurements of the subsolar shock position have been used. The difference between this study and that of Slavin is that more terminator data were used to define the solar cycle variation and that a more appropriate Mach number and ratio of specific heats were used. We also ran the gas dynamic code for many different obstacle shapes to define accurately the functional dependence of the various distances.

Finally, we have measured the location of the subsolar bow shock for the first time, albeit only under low solar activity. This altitude is 2280 km. The results of comparing the inferred solar cycle dependent shape suggests that this altitude is higher at solar maximum.

Acknowledgments. We are grateful to J. R. Spreiter for many useful discussions on the location of planetary bow shocks and to both J. P. Spreiter and S. Stahara for the use of their code. This work was supported by the National Aeronautics and Space Administration under research contract NAS 2-9491.

References

- Brace, L. H., R. F. Theis, W. R. Hoegy, J. H. Wolfe, J. D. Mihalov, C. T. Russell, R. C. Elphic and A. F. Nagy, The dynamic behavior of the Venus ionosphere in response to the solar wind, *J. Geophys. Res.*, **85**, 7663, 1980.
- Fairfield, D. H., Average and unusual locations of the earth's bow shock, *J. Geophys. Res.*, **76**, 6700-6716, 1971.
- Phillips, J. L., J. G. Luhmann and C. T. Russell, Growth and maintenance of large-scale magnetic fields in the dayside Venus ionosphere, *J. Geophys. Res.*, **89**, 10676, 1984.
- Russell, C. T., The Venus bow shock: Detached or attached?, *J. Geophys. Res.*, **82**, 625-631, 1977.
- Russell, C. T. and O. Vaisberg, The interaction of the solar wind with Venus, in *Venus*, (edited by D. M. Hunten, L. Colin, T. M. Donahue and V. I. Moroz), pp. 873-940, University of Arizona Press, Tucson, AZ, 1983.
- Russell, C. T., J. G. Luhmann, R. C. Elphic and F. L. Scarf, The distant bow shock and magnetotail of Venus: Magnetic field and plasma wave observations, *Geophys. Res. Lett.*, **8**, 843-846, 1981.
- Russell, C. T., J. T. Gosling, R. D. Zwickl and E. J. Smith, Multiple spacecraft observations of interplanetary shocks: ISEE three-dimensional plasma measurements, *J. Geophys. Res.*, **88**, 9941-9947, 1983.

- Slavin, J. A., R. C. Elphic, C. T. Russell, J. H. Wolfe and D. S. Intriligator, Position and shape of the Venus bow shock: Pioneer Venus orbiter observations, Geophys. Res. Lett., 6, 901-904, 1979.
- Slavin, J. A., R. C. Elphic, C. T. Russell, F. L. Scarf, J. H. Wolfe, J. D. Mihalov, D. S. Intriligator, L. H. Brace, H. A. Taylor, Jr. and R. E. Daniell, Jr., The solar wind interaction with Venus: Pioneer Venus observation of bow shock location and structure, J. Geophys. Res., 85, 7625-7641, 1980.
- Slavin, J. A., R. E. Holzer, J. R. Spreiter, S. S. Stahara and D. S. Chausee, Solar wind flow about the terrestrial planets, 2. Comparison with gas dynamic theory and implications for solar planetary interactions, J. Geophys. Res., 88, 19, 1983.
- Smirnov, V. N., O. L. Vaisberg and D. S. Intriligator, An empirical model of the Venusian outer environment, 2. The shape and location of the bow shock, J. Geophys. Res., 85, 7651-7654, 1980.
- Spreiter, J. R. and S. S. Stahara, Solar wind flow past Venus: Theory and comparisons, J. Geophys. Res., 85, 7715-7738, 1980.
- Tatrallyay, M., C. T. Russell, J. G. Luhmann, A. Barnes and J.D. Mihalov, On the proper Mach number and ratio of specific heats for modeling the Venus bow shock, J. Geophys. Res., 89, 7381-7392, 1984.
- Winterhalter, D., M. G. Kivelson, R. J. Walker and C. T. Russell, Magnetic field changes across the earth's bow shock: Comparison between observations and theory, J. Geophys. Res., 90, 3925-3933, 1985.
-
- J. G. Luhmann, J. L. Phillips and C. T. Russell, Institute of Geophysics and Planetary Physics, University of California, Los Angeles, California 90024

(Received July 26, 1985;
accepted August 12, 1985.)